HOMOGENIZATION OF METRIC HAMILTON-JACOBI EQUATIONS

ADAM M. OBERMAN, RYO TAKEI, AND ALEXANDER VLADIMIRSKY

ABSTRACT. In this work we provide a novel approach to homogenization for a class of static Hamilton-Jacobi (HJ) equations, which we call metric HJ equations. We relate the solutions of the HJ equations to the distance function in a corresponding Riemannian or Finslerian metric. The metric approach allows us to conclude that the homogenized equation also induces a metric. The advantage of the method is that we can solve *just one auxiliary equation* to recover the homogenized Hamiltonian $\bar{H}(p)$. This is significant improvement over existing methods which require the solution of the cell problem (or a variational problem) for each value of p. Computational results are presented and compared with analytic results when available for piece-wise constant periodic and random speed functions.

CONTENTS

1. Introduction

sec:intro

In this work we provide a novel approach to homogenization for a class of convex Hamilton-Jacobi (HJ) equations, which we call metric HJ equations. We relate the solutions of the HJ equations to the distance function in a corresponding Riemannian or Finslerian metric. By appealing to a homogenization result for metrics, we conclude that the homogenized equation is also the distance in a homogenized metric. The advantage of our method is that we can solve *just one auxiliary equation* to recover the homogenized Hamiltonian $\bar{H}(p)$. This is significant improvement over existing methods which require the solution of the cell problem (or a variational problem) for each value of p.

An application is front propagation problems in multiscale media. The wide separation of spatial scales prohibits the direct solution of the fully resolved problem. Instead, the medium which varies on small scales is replaced by a homogeneous medium, which approximates the propagation of the fronts on the larger scale.

The main theoretical idea is to recognize that the distance function in the homogenized metric captures the solution to a variational problem for the geodesics corresponding to all directions. This distance function, which is approximated by solving a single Hamilton-Jacobi equation, can be used to recover the entire homogenized metric. To make this procedure work, we need to be able to easily translate results for anisotropic front propagation

between various formulations (reviewed in section §2). The first formulation expresses the speed of propagation in the media by a local speed function. The speed function induces a metric on the space, given by the least time to traverse using admissible paths. The distance function in this metric satisfies an eikonal-type Hamilton-Jacobi equation.

Remark. Our results apply to the metric Hamiltonian $H(p, x) = 1$, which homogenizes to $\bar{H}(p)$. We mention here that the results extend to some other cases, provided $H(p, x)$ is a metric Hamiltonian. While it is not completely obvious, it is true that $H^2(\nabla u, x) = 1$ homogenizes to $\bar{H}^2(\nabla u) = 1$. In the time-dependent case, $u_t = H(\nabla u, x)$, homogenizes to $u_t = \bar{H}(\nabla u)$. In addition, $u_t = H^2(\nabla u, x)$ homogenizes to $u_t = \bar{H}^2(\nabla u)$. These results can be obtained using the Hopf-Lax formula. For an explanation, see the remarks at the end of section §2.9 and at the start of section §3.

Another natural definition of metric in an inhomogeneous medium is provided by the *geodesic distance*. In this case a cost function is minimized. over admissible paths (which are not required to have bounded speeds). The relationship between the cost function and the speed function which makes the geodesic metric equal to the metric induces by the speed function is given in §2.8.

In our approach, we compute an approximation to the homogenized Lagrangian $\bar{L}(q)$ for all values of q. The Legendre transform is then applied to obtain $\bar{H}(p)$ for all values of p. In fact, it is often more convenient to solve anisotropic Hamilton-Jacobi equations by semi-Lagrangian numerical methods. In that case, all that is needed is $\bar{L}(q)$, and the additional step of applying Legendre transform can be avoided.

Contents. The remainder of this section introduces anisotropic front propagation, and presents a few model problems. Section §2 reviews front propagation more thoroughly. The HJ equation for the arrival time is derived, and the geodesic distance is presented. The Lagrangian and the Hopf-Lax formula are reviewed. Section §3 contains a review of homogenization and the proof of the main theoretical result. The algorithmic details of our numerical method are provided in section §4, and the numerical results can be found in section §5.

1.1. **Particle speeds and front normal velocities.** Suppose Γ is the initial position of a front which is advancing monotonically, passing through each point only once. In this case the position of the front at time t can be represented by the level set of a single function $T(x)$. If $T(x)$ is the time when the front passes through the point x, then the level-sets of T give subsequent positions of the front. Assume that the normal speed of the front, $F(x, n)$, depends only on the position, x, and normal direction, n. If the front remains smooth, its normal direction is $n = \frac{\nabla T}{|\nabla T|}$ and the rate of increase of T in that direction is equal to $|\nabla T|$. On the other hand, this rate
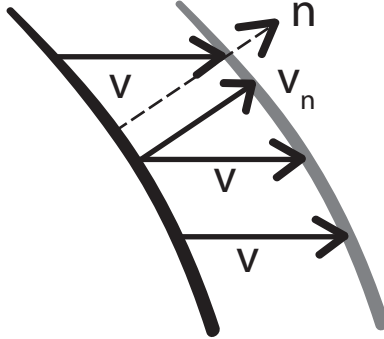
Figure 1: Illustration of normal front speed versus particle speed.   `fig:front`

of increase should be the reciprocal of the normal speed, F. This yields the following static Hamilton-Jacobi equation

$$F\left(x, \frac{\nabla T(x)}{|\nabla T(x)|}\right) |\nabla T(x)| = 1$$

with the boundary condition $T = 0$ on Γ. However, this argument is formal, since the advancing front will generally not remain smooth. (For two growing circles, the front develops a cusp when they intersect.) To deal with singularities, the notion of *viscosity solutions* should be used to interpret this Partial Differential Equation (PDE) [12].

A Lagrangian formulation of the same problem results from considering a front as an aggregate of infinitely many particles, all of which are moving along optimal trajectories, with the goal of advancing in the front's normal direction as quickly as possible. The optimal particle trajectories coincide with the characteristics of the above PDE, and the front remains smooth as long as these optimal trajectories do not intersect.

In order to properly link the Hamilton-Jacobi equation with the Lagrangian formulation, we need to be particularly careful when dealing with anisotropic speeds. In the isotropic case, $F(x, n) = c(x)$ and the optimal direction for particle-travel is also orthogonal to the front, yielding the Eikonal PDE

$$c(x)|\nabla T(x)| = 1.$$

In the anisotropic case, the normal velocity of the front is different from the velocity of the moving particles which make up that front.

Example. Suppose particles move horizontally with speed 1, and have no vertical speed allowed. Then the front with normal $(1,1)/\sqrt{2}$ moves with speed $1/\sqrt{2}$ in the normal direction, whereas the vertical front moves at speed 1 and a horizontal front does not move at all. See Figure 1.

The example above can be extended to the general case, where the allowable particle speed in the direction α is given by $c(x, \alpha)$. All particles try to advance the front as quickly as possible; so the optimal direction for particle-motion will depend on the local orientation of the front. In that case, the normal speed of the front is

$$F(x, n) = \max_{|\alpha|=1}\{(n \cdot \alpha)c(x, \alpha)\},$$

and the maximizing α corresponds to the direction of particle motion. This connection is discussed in detail in section §2.4. Here we simply note that the front-crossing-time function $T(x)$ is the viscosity solution of the Hamilton-Jacobi equation $H(\nabla T(x), x) = 1$, where the Hamiltonian is given by

$$\boxed{\texttt{HfromSpeed}} \quad (1) \qquad H(p, x) := \max_{|\alpha|=1}\{(p \cdot \alpha)c(x, \alpha)\} = |p|F\left(x, \frac{p}{|p|}\right).$$

Before going into the details of our approach, we present several model problems.

1.2. The periodic checkerboard.
Consider a periodic checkerboard, where the speed of motion is either 1 or 2. Suppose further that the scale of the periodicity, ϵ, is too small to resolve computationally. Clearly, simply solving on a coarse grid could produce incorrect results, because the coarse grid could fail to resolve one of the two parts of the medium. This is where *homogenization* comes in: we need to replace the medium which varies on small scales with an approximation which captures the large scale behavior.

The homogenized medium can be found by finding the explicit optimal paths (which are not unique). In this case, if the ratio of speeds is large enough, there is no point spending any time in the slower material. (For horizontal, vertical and diagonal directions, the paths stay in the fast squares, and move directly, up to small oscillations on the scale of ϵ. But other directions, for example the direction $(2, 1)$, there is no straight line path, so the optimal path is longer than in the Euclidean case. As a result, the homogenized speed is slower for these directions. See Figure 2. These heuristic arguments can be made rigorous [1]. The checkerboard medium homogenizes to a medium whose vectogram is octagonal. We represent the speed of propagation by a *vectogram* which illustrates the speed in each possible direction permitted by the material. See Figure 3.) This example illustrates a general principle,

Anisotropy can develop as a result of homogenization.

1.3. The random checkerboard.
The random case, where each square is fast or slow with probability one half, is shown in Figure 4. In this case, numerical results suggest that homogenized material is isotropic with speed faster than the harmonic mean, see section §5.5.
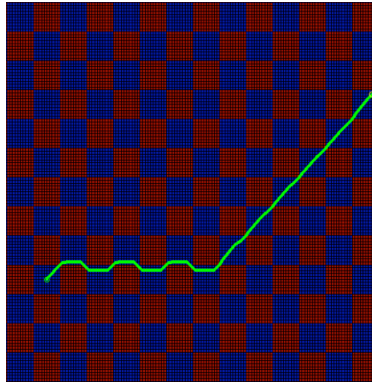
Figure 2: An optimal path in the $(2, 1)$ direction for the checkerboard material.   `fig:path`
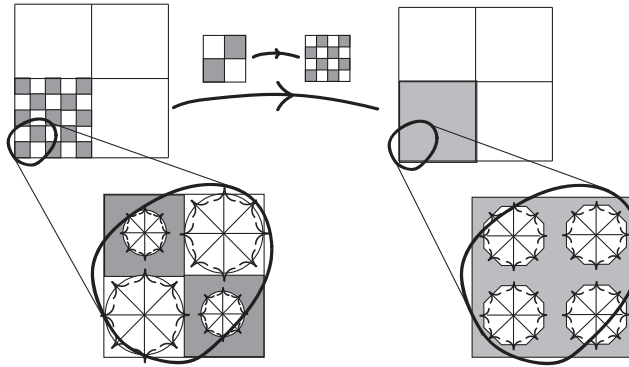
Figure 3: Homogenization of the checkerboard material, illustrated with vectograms.   `fig:checkerboard`

`toy3scale`

1.4. **The toy three scale problem.** Consider a two dimensional material made up of fifty by fifty unit blocks. Each block is allowed to have a different periodic small scale structure. See Figure 5.

To solve the full three scale problem, we apply a two step procedure. First in each block, homogenize to get a homogenous material with a new (anisotropic) speed profile. Next, on the large scale, solve the front propagation problem on a grid which resolves each block, using the speed profile for the homogenized blocks. See Figure 5 and Figure 11. Accurate results can be obtained with a modest number of grid points on each block, see §5.2.
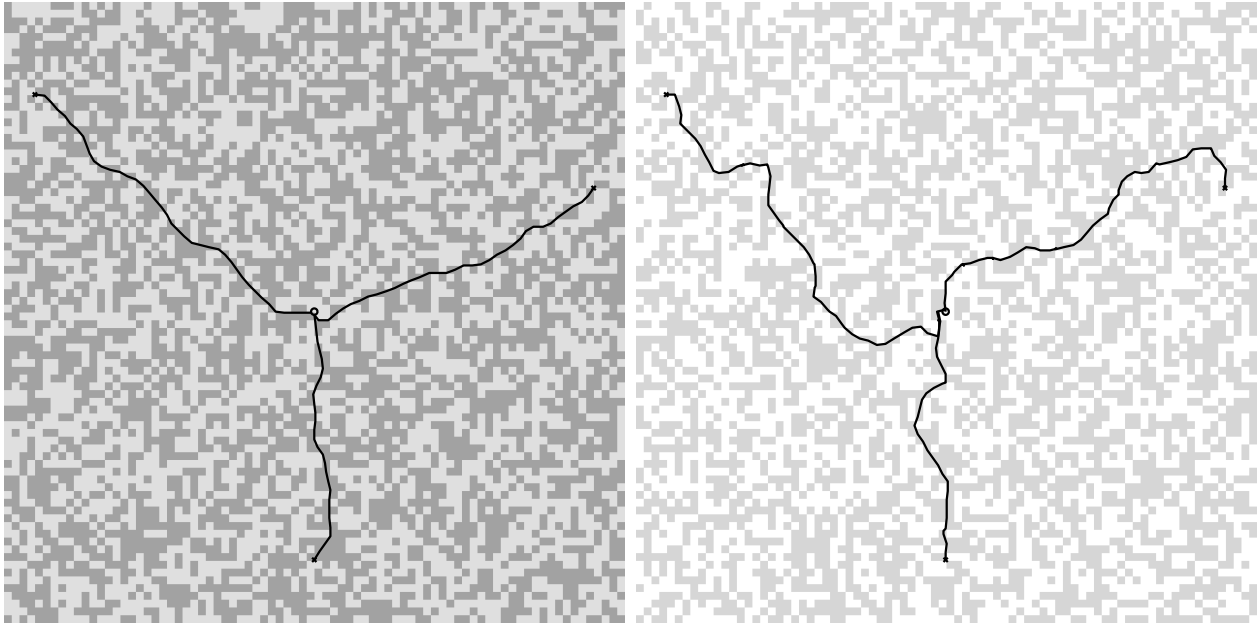
Figure 4: Optimal paths in a random media. The particle speed is $c_0 > 1$ `fig:randomPath`
in the dark and 1 in the light region. Left: $c_0 = 2$. Right: $c_0 = 10$.
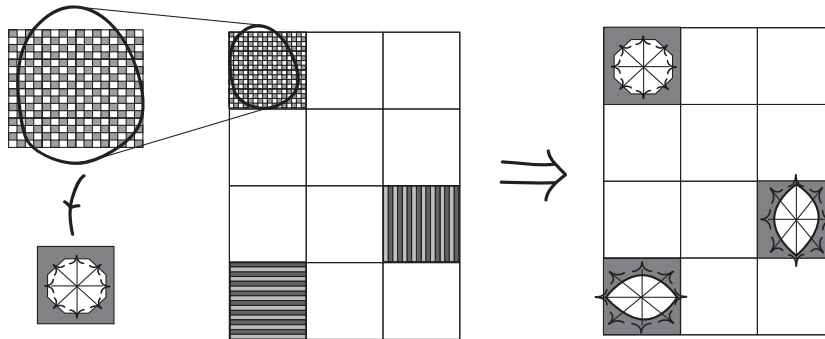
Figure 5: The three scale problem (left), result of homogenization in each   `fig:3scaleSol`
medium scale cell (right)

`sec:fronts`

2. Paths and fronts in an inhomogeneous medium

In this section we review front propagation in an inhomogeneous and anisotropic medium from the perspective of the optimal control theory. We

discuss the least time perspective, and the related Eikonal equation for the distance.

We recall the derivation of the Hamilton-Jacobi equation for the distance function. The distance function is interpreted as the first arrival time for a front given as the envelope of particles moving along the optimal paths at speed given by c. The normal speed of a front is not the same as the particle speed. However, we make the observation in 2.9 that the particle speed function defines a norm, and that the HJ equation for the distance is a generalized eikonal equation in the *dual norm*.

These different interpretations of HJ equations are later used in section §3 to derive an efficient method for homogenization.

`sec:summary`

2.1. Summary of notation and relationship between the variables.

- x is a generic point in $\mathbb{R}^n$ representing position.
- p, q are generic vectors in $\mathbb{R}^n$ representing velocity.
- β is a generic vector in $\mathbb{R}^n$ satisfying $|\beta| \leq 1$.
- α is a generic unit vector in $\mathbb{R}^n$ representing direction.
- $c(x, \alpha)$ is the particle speed in the direction α.
- $f(x, \alpha)$ gives the particle velocity in the direction α, $f(x, \alpha) = \alpha c(x, \alpha)$
- $F(x, n)$ gives the speed for a front with normal n.
- $b(x, q)$ is the cost at x to move with velocity q.
- The vectogram, $V_c(x) = \{f(x, \beta) \mid |\beta| \leq 1\}$ is a set of all permissible velocities at the point x.
- The Hamiltonian, $H(p, x) = |p| F(x, p/|p|)$.
- The Lagrangian $L(q, x) = 0$ if $q \in V_c(x)$, ∞ otherwise.

The normal speed F and particle speed c are related by the homogeneous Legendre Transform [28]. The Hamiltonian, H, and the Lagrangian L are related by the Legendre Transform, see section §2.5. The particle speed c and the metric cost function b are one sided inverse functions, see section §2.8. For each fixed x, the metric cost function b and the Hamiltonian H are norms on $\mathbb{R}^n$. These are dual norm, see section §2.9.

2.2. The speed function, vectograms.
Consider a medium which allows particle motion at limited speeds. Let x denote the position, and β denote the control value. Write $\dot{x}(s, \beta(s)) := \frac{d}{ds} x(s, \beta(s))$. The admissible paths $x(s, \beta(s))$ satisfy the controlled ordinary differential equation

`dynamics`   (ODE) $$\dot{x}(s, \beta(s)) = f(x(s, \beta(s)), \beta(s)),$$

where $\beta(\cdot) \in \mathcal{B} := \{\beta(\cdot) : [0, \infty) \to \mathbb{R}^n, |\beta| \leq 1, \text{ measurable}\}$ is the *control*.

We restrict to the special case where the control is the choice of direction:

`speedfunction`   (2) $$f(x, \beta(s)) = c\left(x, \frac{\beta(s)}{|\beta(s)|}\right) \beta(s).$$

The *speed function* $c : \mathbb{R}^n \times \mathbb{S}^{n-1} \to [0, +\infty)$ gives the maximum speed allowed in the direction α, where $\alpha = \beta(s) |\beta(s)|^{-1}$ is a unit vector. We

assume that c is convex in its second argument and satisfies the small-time controllability condition:

`growth` (3) $\qquad 0 < c_1 \leq c(x, \alpha) \leq C_1 < +\infty \qquad$ for every $x \in \mathbb{R}^n, |\alpha| = 1.$

The function c is *homogeneous* if it is independent of x, $c(x, \alpha) = c(\alpha)$, *isotropic* if it is independent of the direction, α, $c(x, \alpha) = c(x)$, and *symmetric* if

`speedsymmetric` (4) $$c(x, -\alpha) = c(x, \alpha).$$

We assume symmetry to ensure that the resulting distances on $\mathbb{R}^n$, $T_c(x_1, x_2)$, are symmetric, although the assumption can be dropped at the expense of some additional bookkeeping (we would need to distinguish between arrival times, and times to reach a target, some of the formulas will have minus signs in the velocities, see [28] and norms are replaced by asymmetric norms).

For fixed $x \in \mathbb{R}^n$, the speed function c is a mapping of the unit sphere, $\mathbb{S}^n$, and also defines a *vectogram* $V_c \subset \mathbb{R}^n$:

$$V_c = \left\{ c\left(x, \frac{\beta(s)}{|\beta(s)|} \right) \beta \,\middle|\, |\beta| \leq 1 \right\}.$$

Vectograms [20] provide a simple way to illustrate the speed profile for each point x. See Figures 3 and 8.

`sec:arrivaltime`

2.3. The arrival time function.

We can define a distance on $\mathbb{R}^n$ using the minimum time needed to move between two points along the admissible paths:

`ds` (5) $\qquad T_c(x_1, x_2) = \inf_{x(\cdot) \text{ admissible}} \{t \mid x(0) = x_1, x(t) = x_2\}.$

It is easy to show that T_c defines a metric on R^n, where the symmetry property results from the fact that any admissible path from x_1 to x_2 can be retraced backwards taking the same amount of time (using (4)). The small-time controllability condition (3) can be used to show that the infimum is attained and that an optimal (not necessarily unique) control $\beta(s)$ actually exists. Moreover, since the goal is to minimize the time, it is clear that along any optimal path the particle should be moving with the maximum allowable speed for the current direction; i.e., $|\beta(s)| = 1$ and $f(x(s), \beta(s))$ is on the boundary of the vectogram V_c a.e. in $[0, t]$. Thus, the same distance function can be defined by using the class of admissible controls $\mathcal{A} := \{\alpha(\cdot) : [0, \infty) \to \mathbb{R}^n, |\alpha| = 1, \text{ measurable}\}$.

`sec:dist`

2.4. The Hamilton-Jacobi equation.

In this section we show directly that the first arrival time function satisfies the Hamilton-Jacobi equation, using the Dynamic Programming Principle [4]. Here we give a formal proof (assuming the solution remains smooth), for the reader's convenience, and to establish consistent notation. A rigorous treatment (using visosity solutions to handle the non-smoothness) as well as the proof of uniqueness for similar equations can be found in [15] and [4].

The Hamiltonian $H(p, x)$ was defined in equation (1),

<div style="border:1px solid;">lem:1</div> *Lemma* 1. The arrival time to the origin, $T(x) = T_c(x, 0)$, is the viscosity solution to the *Hamilton-Jacobi* equation

<div style="border:1px solid;">hjb</div> (HJ) $$H(\nabla T, x) = 1, \quad T(0) = 0.$$

The Hamiltonian $H(p, x)$ was defined in equation (1).

Proof. Assume that $T(x)$ is smooth and consider all paths, which start from x and move in the constant direction α for a small time h. Define $y_\alpha = x + hc(x, \alpha)\alpha$. Then

$$T(x) = \min_\alpha \{T(y_\alpha) + h + o(h^2)\}$$
$$= \min_\alpha \{T(x) + c(x, \alpha)(\alpha \cdot \nabla T(x)) + h + o(h^2)\}.$$

Subtracting $T(x)$, dividing by h, and taking the limit $h \to 0$ gives

$$-1 = \min_\alpha \{c(x, \alpha)(\alpha \cdot \nabla T(x))\},$$

or $\max_{|\alpha|=1} \{c(x, -\alpha)(\alpha \cdot \nabla T(x)) s\} = 1$ as in (1), where we have used the symmetry of the speed (4). $\qquad\square$

<div style="border:1px solid;">sec:Lagrangian</div>

2.5. **The Lagrangian.** An equivalent way to define the distance, (5), is using the *Lagrangian*,

<div style="border:1px solid;">LagDef</div> (6) $$L(q, x) = \begin{cases} 0 & q \in V_c, \\ \infty & \text{otherwise.} \end{cases}$$

Then the definition of distance (5) can be rewritten as the Hopf-Lax formula [15] for the arrival time function

<div style="border:1px solid;">HopfLax</div> (7) $$T(x) = \inf \left\{ t + \int_0^t L(\dot{x}(s), x(s))\, ds \,\middle|\, x(0) = 0,\ x(t) = x \right\},$$

where the infimum is over $W^{1,1}((0, t); \mathbb{R}^n)$. For consistency, we verify that the Hamiltonian $H(p, x)$ is obtained from the Lagrangian via the Legendre transformation [15]

$$H(p, x) = L^*(p, x) = \max_q \{p \cdot q - L(q, x)\}$$
$$= \max_{q \in V_c} \{p \cdot q\}$$
$$= \max_{|\alpha|=1} \{(p \cdot \alpha)\, c(x, \alpha)\}.$$

2.6. **Isotropic speeds.** The optimal particle trajectories are given by the characteristics of the Hamilton-Jacobi equation. In the anisotropic case, the normal speed $F(x, n)$ is given by (1),

$$F(x, n) = \max_{|\alpha|=1} \{(n \cdot \alpha)\, c(x, -\alpha)\}.$$

When $c(x, \alpha) = c(x)$ is isotropic, then $F(x, n) = c(x)$. and $H(p, x) = |p|c(x) = 1$, which is an Eikonal equation. In this case, the characteristic curves coincide with the gradient lines of the viscosity solution, yielding

$$n = \frac{\nabla T(x)}{|\nabla T(x)|}.$$

In the special case where the speed function is homogeneous, $c(x, \alpha) = c(\alpha)$, the optimal paths are straight lines, and the arrival time to a point is simply given by the ratio of the distance to the speed.

$\boxed{\texttt{TimeHomog}}$ (8) $\qquad T(x) = \dfrac{|x|}{c(x/|x|)}, \qquad$ when $T(0) = 0$ and $c(x, \alpha) = c(\alpha)$

For the more general boundary condition $T(x) = g(x)$ on Γ, we obtain

$\boxed{\texttt{homogenized\_from\_Gamma}}$ (9) $\qquad T(x) = \min\limits_{y \in \Gamma} \left\{ \dfrac{|x - y|}{c\left(\frac{x-y}{|x-y|}\right)} + g(y) \right\}.$

$\boxed{\texttt{sec:geodesic}}$

2.7. **The geodesic distance.** We review the notion of geodesic distance in this context, and below we will relate it to Hamilton-Jacobi equations. The link between Hamilton-Jacobi equations and metrics has been observed before. We refer to [29] and the references therein.

We are given a metric cost function, $b(x, q)$ which is positively 1-homogeneous in the second variable,

$\boxed{\texttt{1homogfc}}$ (10) $\qquad b(x, tq) = tb(x, q), \qquad$ for every $(x, q) \in \mathbb{R}^n \times \mathbb{R}^n$ and $t > 0$.

This will ensure that the distance defined below is invariant under change of parameterizations of the path. In addition, we assume that b is convex in the second variable and satisfies the growth condition:

$\boxed{\texttt{growthfc}}$ (11) $\qquad c_2|q| \le b(x, q) \le C_2|q|, \qquad$ for every $(x, q) \in \mathbb{R}^n \times \mathbb{R}^n$,

with $0 < c_2 \le C_2 < +\infty$. Under the assumptions (10) and (11), the cost function defines a norm on $\mathbb{R}^n$, for each x,

$\boxed{\texttt{Fcnorm}}$ (12) $\qquad\qquad\qquad\qquad \|q\|_b = b(x, q).$

We also assume that $b(x, q) = b(x, -q)$, which ensures the distance is symmetric, $d_b(x_1, x_2) = d_b(x_2, x_1)$.

Given a path $x(\cdot) \in W^{1,1}((0, t); \mathbb{R}^n)$, the total cost of the path is

$\boxed{\texttt{Jdefn}}$ (13) $\qquad\qquad\qquad J[x(\cdot)] = \int_0^t b(x(s), \dot{x}(s))\, ds.$

The geodesic distance between two points is the minimal cost

$\boxed{\texttt{geodesic}}$ (14) $\qquad d_b(x_1, x_2) = \inf \{J[x(\cdot)] \mid x(0) = x_1,\ x(t) = x_2\}$

where the infimum is over $x(\cdot) \in W^{1,1}((0, t); \mathbb{R}^n)$.

Remark (Riemannian and Finslerian metrics). If the cost function is given by the square root of a convex quadratic function, i.e.

$$b(x, \alpha) = \sqrt{g_{ij}(x)\alpha_i\alpha_j},$$

for $g(x)$ a symmetric positive definite matrix, the resulting metric, d_b, is Riemannian. (In that case the vectograms V_c are ellipses.) Otherwise, d_b is a *Finslerian* metric [29].

Remark (Non-differentiable geodesics). In a Finslerian metric, geodesics need not be differentiable, as is the case for the octagon norm. See [9][3] for more information on Finslerian metrics. The distance function may also be non-differentiable.

sec:relating

2.8. **Relating the geodesic metric and the arrival time.** So far we have defined two distances. The arrival time, $T_c(x_1, x_2)$, (5), is the arrival time using paths which move at speed admissible by the speed function $c(x, \alpha)$. The geodesic distance, $d_b(x_1, x_2)$, (14) is the minimal cost of paths, where the cost is measured using the metric cost function $b(x, p)$. The two distances are equal if the metric cost function and the particle speed function are (one-sided) inverses.

lem:2   *Lemma* 2. The distances defined by (5) and (14), respectively, are equal,

distequal   (15) $$T_c(x_1, x_2) = d_b(x_1, x_2),$$

provided that the speed function, c, and the cost function, b, are related by

fcdefn   (16) $$b(x, c(x, \alpha)\alpha) = 1, \quad \text{for all } |\alpha| = 1, x \in \mathbb{R}^n,$$

with the remaining values of b determined by homogeneity (10).

Proof. We argue formally, assuming the infimum in the definitions is achieved by differentiable paths. The proof can be made rigorous by approximation. Given $x_1, x_2 \in \mathbb{R}^n$, suppose $T_c(x_1, x_2) = t$ and $d_b(x_1, x_2) = s$.
     First let

$$x(\cdot) : [0, t] \to \mathbb{R}^n, \quad x(0) = x_0, \ x(t) = x_1.$$

be an admissible curve for the speed function c. Then $x(\cdot)$ satisfies (ODE), and $T_c(x_0, x_1) = t$. Compute the integral in the definition (14) using the path $x(\cdot)$. Then by (ODE), $\dot{x}(s) \in V_c$. Furthermore, we can assume that $\dot{x}(s) \in \partial V_c$, since otherwise the curve could be made faster. Thus by (16), $b(x, \dot{x}) = 1$, so $s \leq t$.
     Next let $x(\cdot)$ be a curve from x_1 to x_2 for which the cost $J[x(\cdot)] = s$. We can find a parameterization of the path by arclength, i.e. a path $y(\cdot)$, for which $b(y(s), \dot{y}(s)) = 1$. Then by (16), $\dot{y}(s) \in V_c$, the vectogram at $y(s)$, so $y(\cdot)$ is an admissible path for the distance function T_c. Thus $t \leq s$.   □

A similar proof of this property can be also found in [30].

`sec:dualnorm`

2.9. **Dual Norms, The Eikonal equation.** We show that (HJ) can be rewritten as an Eikonal equation in a suitable norm. This relates the speed or cost functions to the normal velocity.

We refer to [6][Appendix 1.1.6] for material on norms and dual norms. A closed, bounded set with non-empty interior, e.g. V_c, can be used to define a norm (by using the set as the norm ball and extending by homogeneity) provided the set is symmetric about the origin, and convex. Convexity of the set ensures the triangle inequality for the norm.

Given a norm $\| \cdot \|$ on $\mathbb{R}^n$, the dual norm $\| \cdot \|_*$ is defined as

`dualnorm`   (17) $$\|x\|_* = \max\{x \cdot y \mid \|y\| = 1\}.$$

Then $\|x\|_{**} = \|x\|$.

Example. The p-norms $\|x\|_p = (\sum_{i=1}^n |x|^p)^{1/p}$ are dual to the q norms, with $1/p + 1/q = 1$ for $1 \le p \le \infty$. This follows from Hölder's inequality on $\mathbb{R}^n$, $x \cdot y \le \|x\|_p \|y\|_q$. In particular this is true for $p = 1$ and $p = \infty$, where the norm balls are diamonds and squares. Generalizing this case, dual polygonal norms can be obtained as well. For example, the dual of the norm $\|x\| = \max(|x_1|, |x_2|, |x_1 + x_2|)$, is the norm $\|x\|_* = \max(|x_1|, |x_2|, |x_1 - x_2|)$

Write, for fixed x, the dual norm

$$\|p\|_{b*} := \max\{p \cdot q \mid \|q\|_b = 1\}$$
$$= \max_{|q|=1}\{p \cdot q\, c(x,p)\}.$$

by (16). Thus equation (HJ) is equivalent to

`anieik`   (Eikonal) $$H(\nabla T(x), x) = \|\nabla T(x)\|_{b*}.$$

If we are given the Hamilton-Jacobi equation $H(p, x)$ which is positive 1-homogeneous in p for each x, we can recover the cost function by taking the dual

`fcfromH`   (18) $$\|q\|_b = \max_p\{q \cdot p \mid H(p, x) = 1\}.$$

The Legendre transform of the norm $\|\cdot\|_{b*}$ is the dual norm unit ball [6][pg 93], which gives the vectogram.

Remark. In general it is not true that homogenizing and squaring commute. The reason that the results of [10] (for eikonal squared) and [11] (for eikonal) give equivalent homogenized values, is that the Legendre transform of a norm is the indicator set of the dual norm, while the Legendre transform of a norm squared is the dual norm squared (see [6] example 3.26 and 3.27).

3. HOMOGENIZATION

`sec:homog`

3.1. **Homogenization background.** Theoretical works on homogenization provide existence results and convergence rates for the solution of the homogenization problem. We mention the early unpublished work [22] for

Hamilton-Jacobi equations, and refer to the textbooks, [23] for linear equations, and [7], for homogenization of HJ equations and Riemannian metrics [pp142–145]. A list of more detailed references can be found in the review [14]

Explicit analytic solutions for several examples can be found in [10]. A series of examples in the time dependent front propagation case, can be found in [11]. Both works find explicit solutions by homogenizing the Lagrangian, refer to sections §3.4 and §2.5. The first work used Hamiltonians which are homogeneous order two in p, ($H(p,x)^2$ in our notation), and so the resulting Lagrangian was also homogeneous order two in p. The second work used a time-dependent equation, with a similar Hamiltonian to the one herein. In both cases, the Lagrangian is related to the Hamiltonian by the Legendre transform.

The cell problem (section §3.3) can be solved numerically to compute $\bar{H}(p)$. This was done for front propagation in [21], and for more general Hamiltonians in [24] and [25]. There are other methods for computing $\bar{H}(P)$, see [16].

3.2. **Homogenization in one dimension.**

Example. For the case of front propagation in a one-dimensional periodic medium, it is not difficult to show that the homogenized speed function is the harmonic mean of the speed function over a periodic cell. Suppose our one dimensional domain consists of ϵ-intervals with the speed alternating between 1 and 5. Then the travel times in these materials are 1 and 1/5, so the total time for the front to traverse the entire domain is 3/5, and the average speed is 5/3, the harmonic mean of 1 and 5.

To obtain this result formally for the Hamilton-Jacobi equation, we go through the following procedure. (i) rewrite $c(x)|T_x| = 1$, as $|T_x| = c(x)^{-1}$, (ii) average the reciprocal of the speed function (iii) divide by the averaged coefficient, to obtain

$$\frac{1}{\text{average of } c(x)^{-1}}|T_x| = 1.$$

Remark. This heuristic is quite similar to the one used when homogenizing linear equations, but it is not directly applicable to HJ equations in higher dimensions. To obtain the total cost to travel from x_0 to x_1 the cost is integrated along the optimal trajectory, (which need not be a straight line). The homogenized cost for that direction is then obtained by dividing the total cost by $|x_0 - x_1|$. The cost has units of inverse speed, the average cost is the time divided by the distance.

sec:cell

3.3. **The cell problem for Hamilton-Jacobi equations.** In this section we outline the cell problem. A precise statement of a typical theorem can be found, for example, in [8], or in the review [14]. The cell problem is derived using a formal asymptotic expansion, typical examples of which can be found in Chapter 5 of [18].

Let $H(p, x)$ be a Hamiltonian with is periodic on the cube $[-1, 1)^n$. Let $T^\epsilon(x)$ be the solution of

$$H\left(\nabla T^\epsilon(x), \frac{x}{\epsilon}\right) = 1$$

with $T^\epsilon(0) = 0$. We are interested in the limit $\epsilon \to 0$. Formally expand the solution, T^ϵ, in ϵ, $T(x) = T^0(x, x/\epsilon) + \epsilon T^1(x, x/\epsilon) + o(\epsilon^2)$. Additional arguments which we skip show that we can assume

$$T^\epsilon(x) = T^0(x) + \epsilon T^1(x/\epsilon) + o(\epsilon^2).$$

Inserting the expansion into the equation, and collecting terms of $O(1)$ gives

$$H\left(\nabla_x T^0 + \nabla_y T^1, y\right) = 1,$$

where $y = x/\epsilon$. The variable in this last equation is y, so $\nabla_x T^0 = p$, an unknown constant. The left hand side of the previous equation is a function of y, while the right hand side is constant. Thus we have a solvability condition: we need to find a periodic function $v(y)$, and a vector p which solve the cell problem

$$H(p + \nabla v, x) = 1.$$

Then we can define

$$\bar{H}(p) = 1,$$

for that p, and extend $\bar{H}$ to other values along the line $q = tp$ by homogeneity. According to the theorem, T^ϵ converges (uniformly on compact subsets, possibly with a rate) to the solution of

$$\bar{H}(\nabla T) = 1.$$

3.4. **Variational formulation for fronts.** For time-dependent fronts, a variational formulation of the homogenization problem was used in [11]. This is based on the Lagrangian formulation of the problem, and the convergence is in the sense of Γ-convergence [7]. The variational problem takes the form

$$\bar{L}(q) = \liminf_{T\to\infty} \frac{1}{T} \inf_{\phi \in H_0^1(0,T)} \int_0^T L(qt + \phi(t), q + \dot{\phi}(t))\, dt.$$

In this case, the minimization is performed for each value of q, and the Hamiltonian $\bar{H}(p)$ is recovered via the Legendre transform. The resulting Hamiltonian is homogeneous of order one in the gradient, and the Lagrangian is a characteristic function, as in (6). We note that the discontinuous nature of the Lagrangian limits the usefulness of this approach for numerical approximation.

3.5. Homogenization of metrics.

In this section, we review a homogenization result for the geodesic distance functional.

We use the result from [2]. Consider the metric cost functional (13). In addition to (10) and (11), in this section we also assume that $b(\cdot, q)$ is $[-1, 1)^n$ periodic for every $q \in \mathbb{R}^n$. Then for every $\epsilon > 0$, set

$$J^\epsilon[x(\cdot)] = \int_0^t b\left(\frac{x(s)}{\epsilon}, \dot{x}(s)\right) \, ds,$$

According to the theorem from [2], J_ϵ Γ-converges on $W^{1,1}\left((0,t); \mathbb{R}^n\right)$ (in the L^1-topology) to the function defined by

$$J[x(\cdot)] = \int_0^t \bar{b}(\dot{x}(s)) \, ds.$$

Here $\bar{b} : \mathbb{R}^n \to [0, +\infty)$ is 1-homogeneous convex function which also satisfies (11) and is given by

barf   (19) $$\bar{b}(q) = \liminf_{\epsilon \to 0^+ \, x(\cdot)} \left\{ \int_0^t b\left(\frac{x(s)}{\epsilon}, \dot{x}(s)\right) \, ds \mid x(0) = 0, x(t) = q \right\},$$

where again the infimum is over $x(\cdot) \in W^{1,1}\left((0,t); \mathbb{R}^n\right)$.

3.6. Main Homogenization Result.

It is too costly to use the formula (19) which requires the solution of a path minimization problem for each direction q. However, if we knew the homogenized Hamiltonian, we could read it off from the solution of the equation for the first arrival time to the origin $(\overline{HJ})$. But we can approximate this solution by the solution of the inhomogeneous small ϵ equation (HJ^ϵ). This results in an efficient method for $\bar{H}(p)$ We record this result in Theorem 1. See Figure 6 for an illustration of the result, taken from a computation.

Definition 1. The Hamiltonian $H(p, x) : \mathbb{R}^n \times \mathbb{R}^n \to \mathbb{R}$ is a *metric* or *generalized eikonal* Hamiltonian if for each fixed x, $H(\cdot, x) : \mathbb{R}^n \to \mathbb{R}$ satisfies the following

$$H(\cdot, x) \text{ is convex}$$
$$H(tp, x) = tH(p, x) \text{ for all } t \geq 0$$
$$c|p| \leq H(p, x) \leq C|p|$$

with $0 < c_2 \leq C_2 < +\infty$.

We write the equation for the small scale Hamiltonian as

HJe (HJ^ϵ) $$\begin{cases} H\left(\nabla T^\epsilon(x), \frac{x}{\epsilon}\right) = 1, \\ T^\epsilon(0) = 0, \end{cases}$$

and record the homogenized Hamiltonian as

HJb $(\overline{HJ})$ $$\begin{cases} \bar{H}(\nabla T(x)) = 1, \\ T(0) = 0. \end{cases}$$
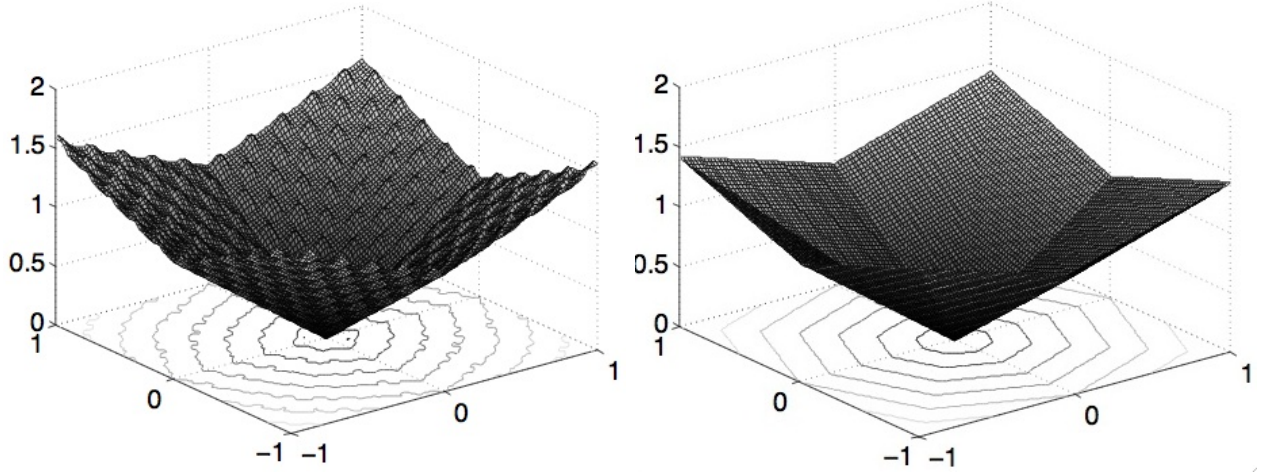
Figure 6: The arrival time $T^\epsilon(x)$ using the periodic cost function $b(x/\epsilon, p)$ converges to the arrival time $T(x)$ with the homogenized cost $\bar{b}(p)$. `fig:cones`

Definition 2. The Hamiltonian $H(p, x)$, which is periodic on the hypercube $[-1, 1)^n$ *homogenizes* to $\bar{H}(p)$ if the viscosity solution $T^\epsilon(x)$ of the Hamilton-Jacobi equation (HJ^ϵ) converges uniformly on compact subsets to the viscosity solution $T(x)$ of $(\overline{HJ})$.

`thm:HJ`   **Theorem 1.** *Let $H(p, x)$ be a metric Hamiltonian which is periodic on the unit hypercube. The function $H(p, x)$ defines a distance on $\mathbb{R}^n$. We can write*

$$H(p, x) = \max_{|\alpha|=1}\{(p \cdot \alpha)c(x, \alpha)\} = \|p\|_{b*}$$

where $c(x, \alpha)$ is the particle speed, $b(x, p)$ is the metric cost function, and the subscript $*$ indicates the dual norm. Then $H(p, x)$ homogenizes to $\bar{H}(p)$ which is a homogeneous metric Hamiltonian, given by

`HJbar`   (20)
$$\bar{H}(p) = \max_{\|\alpha\|=1}\{(p \cdot \alpha)\bar{c}(\alpha)\} = \|p\|_{\bar{b}*}$$

where $\bar{c}(\alpha)$, $\bar{b}$ are the homogenized speed and cost functions, respectively. These functions can be obtained from the arrival time function in the homogenized metric

`fcbar`   (21)
$$\bar{b}(q) = \frac{1}{\bar{c}(q)} = \frac{T(q)}{|q|},$$

and are approximated by

`rate`   (22)
$$\bar{b}(q) = \frac{1}{\bar{c}(q)} = \frac{T^\epsilon(q)}{|q|} + O(\epsilon),$$

where T^ϵ is the solution of (HJ^ϵ).

Remark (Convergence rate)*.* The convergence rate (22) is useful computationally, because we can use Richardson extrapolation in ϵ to better approximate $T(x)$.

This result is obtained from translating freely between the various formulations of the front propagation problems, as summarized in §2.1 and as explained in the earlier sections.

Proof. We begin with the definition of H in terms of the particle speed (1)

$$H(p, x) := \max_{\|\alpha\|=1} \{(p \cdot \alpha)c(x, \alpha)\}.$$

Since $H(p, x)$ is a metric Hamiltonian, we can recover the cost function $b(x, p)$ from the Hamiltonian using the dual norm formula (18)

$$b(x, q) = \|q\|_b = \max_p \{q \cdot p \mid H(p, x) = 1\}.$$

By Lemma 1, the solution $T^\epsilon(x)$ of the Hamilton-Jacobi equation (HJ^ϵ) is the arrival time from the origin using admissible speeds c^ϵ, given by (5)

$$T^\epsilon(x) = \inf_{x(\cdot)} \{t \mid x(0) = 0, \ x(t) = x, \ x(\cdot) \text{ admissible for } c^\epsilon(x, \alpha) \}.$$

Using Lemma 2 in Section §2.8, this is equal to the distance in the b^ϵ metric,

$$T^\epsilon(x) = \inf_{x(\cdot)} \left\{ \int_0^t b^\epsilon(x(s), \dot{x}(s)) \ ds \ \middle| \ x(0) = 0, \ x(t) = x \right\},$$

for $x(\cdot) \in W^{1,1}((0, t); \mathbb{R}^n)$.

At this stage, we appeal to the convergence result for metrics, [2], which is summarized in Section §3.5. The functionals, J^ϵ, Γ-converge to the homogenized cost functional, J. The cost function, $b^\epsilon(x, q)$, converges to a cost function, $\bar{b}(q)$, which is also homogeneous of order one. The minimizing paths $x^\epsilon(\cdot)$ are minimizers of the functionals, and converge in the L^1-topology to the minimizer of the homogenized functional. The distances in the metric $T^\epsilon(x)$ are the minimum values of the functional for paths from the origin to the point x. The values $T^\epsilon(x)$ converge (in $\mathbb{R}$) to $T(x)$ over the minimizing sequences x^ϵ as $\epsilon \to 0$.

Again using Lemma 2, we can write the distance, $T(x)$, in the homogenized metric $\bar{b}$ as the solution of the Hamilton-Jacobi equation for the homogenized cost (20), which gives the last equality in (20),

$$\bar{H}(p) = \|p\|_{\bar{b}*}.$$

If we know $\bar{H}(p)$, we can recover the speed function from the cost function using (18) (actually the formula for the inverse), giving the second equality in (20),

$$\bar{H}(p) = \max_{\|\alpha\|=1} \{(p \cdot \alpha)\bar{c}(\alpha)\}.$$

Since these functions are convex, the optimal path is a straight line, in the directions $\alpha = x/|x|$. Then the travel time for a particle is simply the distance over the particle speed (8)

$$\boxed{\texttt{cbareq}} \quad (23) \qquad\qquad T(x) = \frac{|x|}{\bar{c}(x/|x|)}$$

which gives the second equality in (21).

The convergence of metrics result is useful because it ensures that the $\bar{H}$ is also a metric Hamiltonian. However, to obtain the convergence rate (22), we appeal to results which apply in the more general context of homogenization of period Hamilton-Jacobi equations. We can apply the result of [8], if we transform our equation using the *Kruzkov transformation*: $T^\epsilon(x) = -\log(1 - v^\epsilon(x))$. The result is the convergence rate (22),

$$T(x) = T^\epsilon(x) + O(\epsilon). \qquad\qquad \square$$

4. The Numerical Method

In this section we present our numerical method for homogenization. For the sake of notational simplicity, the method is described in two dimensions, but the generalization to higher dimensional problems is straightforward.

The first step of our algorithm solves (HJ^ϵ) to obtain an approximation to the homogenized speed and cost functions, $\bar{c}(\alpha), \bar{b}(q)$, using (22) in Theorem 1, see sections 4.1 and 4.3. If we are only interested in solving $(\overline{HJ})$, then the solution is provided by (23). If instead, we want to solve $\bar{H}(\nabla T) = 1$ with general boundary conditions, then the solution can be recovered from (9), or it can be obtained numerically. While the analytical formula is useful for evaluating the solution at one point, it is more efficient to solve the equation numerically on a coarse grid, see section 4.4, if the values of the solution on a domain are required.

By combining multiscale problems with different homogenized Hamiltonians in different regions, we solve a toy three scale problem in §5.2, with minor modifications of the method outlined in section §4.4.

To summarize, the complete algorithm consists of two steps: the first is to compute the homogenized speed function $\bar{c}(\alpha)$ for all unit vectors α on the small scale, and the second is to use the homogenized speed function to solve numerically for $T(x)$ on the large scale.

4.1. **Computing the homogenized speed function.** Our plan for computing $\bar{c}(\alpha)$ is based on the formula (21) in §3.

- INPUT: speed function $c^\epsilon(x, \alpha)$.
- OUTPUT: $\bar{c}(\alpha)$, the approximation to the homogenized speed in the direction α.

(A1) Choose $0 < h \ll \epsilon \ll 1$. Numerically solve (HJ^ϵ) on a uniform cartesian grid on $Q = [-1, 1]^2$ with spatial resolution h.

(A2) Choose k vectors $\{q_i\}_{i=1}^k$, which lie on the grid and are of length close to unity, and whose directions $\alpha_i = \frac{q_i}{|q_i|}$ are nearly equally distributed on the circle. Approximate $\bar{c}$ on the grid directions, using (21)

$$\bar{c}\,(\alpha_i) := \frac{|q_i|}{T^\epsilon(q_i)}, \quad i = 1, ..., k.$$

(A3) Interpolate the values $\{\bar{c}(\alpha_i)\}_{i=1}^k$ to approximate $\bar{c}(\alpha)$ for all directions α.

4.2. **Numerical Solution of the HJ equation.** Equation (HJ^ϵ) can be solved by standard methods. In the isotropic case, $c^\epsilon(x, \alpha) = c^\epsilon(x)$, the PDE is Eikonal, which makes both Fast Marching [27] and Fast Sweeping [31] methods directly applicable. A computational comparison of fast marching and fast sweeping approaches to Eikonal PDEs can be found in [19, 17].

Since the discretization of (HJ^ϵ) uses a relatively fine grid, the computational efficiency of the method used to obtain the discretized solution is important. The Fast Marching Method computes the numerical solution in $O(M \log M)$ operations, where the total number of gridpoints is $M = O(h^{-n})$, in $\mathbb{R}^n$, regardless of how oscillatory $c^\epsilon(x)$ is. On the other hand, the number of sweeps needed in the fast sweeping method is proportional to the number of times the characteristics switch their direction from quadrant to quadrant. As a result, the highly oscillatory nature of $c^\epsilon(x)$ mean that the Fast Sweeping Method will require many more sweeps that in the constant c^ϵ case.

In the more general case where c^ϵ is anisotropic, the step (A1) can be carried out using Ordered Upwind Methods [28].

sec:ENO

4.3. **ENO interpolation of vectograms.** We use a second-order essentially non-oscillatory (ENO) method for interpolation. The ENO method can exactly interpolate piecewise quadratic functions. This class matches the shape of the vectograms corresponding to the homogenized speed functions. See Figure 7. In particular, since it can capture vectograms with corners, the ENO method is suitable for approximating not only Riemannian, but also general (Finslerian) metrics.
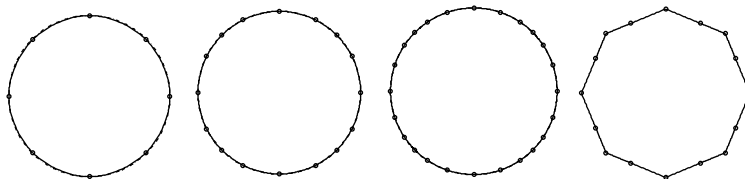

Figure 7: Interpolation using ENO. Interpolated circle, using 8, 16, and 24 points. Interpolated octagon using 16 points.   fig:ENOcircle

The second order ENO method works as follows. Order the unit vectors $\{\alpha_i\}$ in the counter-clockwise direction. Interpolate $\{\bar{c}(\alpha_i)\alpha_i\}$ between $i = j$ and $j + 1$ as follows. Write

$$\bar{c}(\alpha_i)\alpha_i = (x_i, y_i)$$

We describe the case where x_i is the independent variable, which should be applied where $|x_j - x_{j+1}|$ is not too small. The case where y_i is the independent variable follows similarly, where $|y_j - y_{j+1}|$ is not too small.

Step 1 Find the interpolating quadratics

$$h_1(x) = a_1x^2 + a_2x + a_3, \qquad h_1(x_i) = y_i, \qquad i = j - 1, j, j + 1,$$
$$h_2(x) = b_1x^2 + b_2x + b_3, \qquad h_2(x_i) = y_i, \qquad i = j, j + 1, j + 2.$$

Step 2 If $|a_1| < |b_1|$, choose $h_1(\alpha)$ as the interpolating function between $\bar{c}(\alpha_j)\alpha_j$ and $\bar{c}(\alpha_{j+1})\alpha_{j+1}$. Otherwise, choose $h_2(\alpha)$ as the interpolating function.

Remark. We interpolate in Cartesian coordinates, not polar coordinates, even though the latter appears simpler. This method has the special advantage that it captures piecewise linear vectograms exactly, which the polar coordinate version does not.

4.4. **Solving the homogenized equation on a coarse grid.** The homogenized PDE can be written as

$$\bar{H}(\nabla T) = \max_{|\alpha|=1}\{(\alpha \cdot \nabla T)\bar{c}(\alpha)\} = 1.$$

Given $\bar{c}$, formula (8) provides the solution of this PDE on Ω with the boundary condition $T(0) = 0$. As was stated earlier, the solution of $\bar{H}(\nabla T) = 1$ with general boundary conditions can be recovered from (9). However, a good approximation to $T(x)$ can be obtained more efficiently by solving this PDE numerically on a coarse grid in Ω.

Remark. The availability of $\bar{c}(\alpha)$ makes semi-Lagrangian discretizations of the homogenized Hamilton-Jacobi PDE particularly attractive. (Any Eulerian discretization would require an extra step of approximating the dual norm to $\bar{b}$.) Fast non-iterative methods are available for many semi-Lagrangian discretizations. If a finite list of directions of motion is well-represented on a large-scale grid, this results in an auxiliary grid-based graph with positive edge-weights. As a result, the shortest path problem can be solved on that graph using a non-iterative Dijkstra's methods, section §4.5. A more accurate semi-Lagrangian discretization, spanning all possible directions of large-scale motion, was also shown to posses similar causal properties, resulting in related non-iterative Ordered Upwind Methods described in [28].

4.5. **A graph-based discretization of Ω.** We implement a discrete analogue of the dynamic programming principle, where the optimal path is approximated by piecewise linear paths on a finite set of nodes in Ω. We

embed a network X in Ω consisting of a finite node set $V \subset \Omega$ and weighted directed edges $E \subset V \times V$. For each $x \in V$, the neighbors of x form the set

$$\mathcal{N}(x) = \{y \in V : (x, y) \in E\}.$$

We call the set

$$\mathcal{C}(x) = \{y - x : y \in \mathcal{N}(x)\},$$

the *local connectivity* of X at $x \in V$. Construct X so that for all $x, y \in V$

$$y \in \mathcal{N}(x) \Leftrightarrow x \in \mathcal{N}(y),$$

and generally,

$$|v| \text{ is small for all } v \in \mathcal{C}(x), x \in V.$$

The latter condition allows for more accurate approximation of the optimal trajectories (and consequently of the value function) by piecewise linear paths. Naturally, the metric between two adjacent nodes are assigned as the (directed) edge weights. The shortest path problem on a network can then be efficiently solved using Dijkstra's method [13] or by a variant of a Fast Sweeping Method.

- INPUT: $\bar{c}(\alpha)$ from phase one of the algorithm.
- OUTPUT: $\tilde{T}$, the discrete approximation to the $T(x)$ defined on V.

(B1) For each $e_i = (x, y) \in E$ assign a positive edge weight

$$w_i = w(x, y) = |y - x|/\bar{c}\left(\frac{y - x}{|y - x|}\right).$$

(B2) Initialize:

$$\tilde{T}^0(x) = \begin{cases} g(x) & \text{if } x \in V \cap \Gamma, \\ \infty & \text{if } x \in V \backslash \Gamma. \end{cases}$$

(B3) Use either Dijkstra's algorithm or the Fast Sweeping Method to compute *the value function* $\tilde{T}(x)$ (i.e., the least cost to travel from $V \cap \Gamma$ to a node x using the edges in E) for all $x \in V \backslash \Gamma$.

The value function satisfies the following system of discretized equations

| value_func | (24) | $$\tilde{T}(x) = \max_{y \in \mathcal{N}(x)} \left\{w(x, y) + \tilde{T}(y)\right\}, \qquad \forall x \in V \backslash \Gamma.$$ |

If $M = |V \backslash \Gamma|$ and $k = \max |\mathcal{N}(x)|$, Dijkstra's method solves this system in $O(kM \log M)$ operations.

Choice of grid directions q_i and network X. Using Dijkstra's algorithm (B1) - (B3) to approximate the value function, step (A3) may be omitted by carefully choosing the grid directions q_i (in (A2)) and network X.

For example, consider the network where the vertices V are given by uniform cartesian discretization of Ω with refinement h, and for each interior node, the neighbors are the eight closest nodes,

$$\mathcal{C} = \mathcal{C}(x) = \{(\pm h, 0), (\pm h, \pm h), (0, \pm h)\}.$$

Then by choosing the grid directions

$$q_i = v_i/h \text{ where } v_i \in \mathcal{C}, \quad i = 1, \ldots, 8,$$

in the step (A2), we can avoid the interpolation step (A3), since the values at the grid directions are the only values needed to compute the weights in (B1).

However, this introduces an additional error, because the paths used for computing the metric in (19) are being restricted to those which are piece-wise linear with slopes corresponding to the grid directions. This error can be reduced by using more grid directions.

Alternatively, the use of a more accurate semi-Lagrangian discretization described in [28] will automatically minimize over all possible directions of motion, but with that approach the step (A3) becomes unavoidable.

Extension to piecewise-periodic problems. Our algorithm generalizes naturally to problems with multiple regions, each with different periodic structure. Suppose $\Omega = \bigcup_{i=1}^{k} \Omega_i$ is a (finite) partition of the domain, where each Ω_i is equipped with a speed function $c_i^{\epsilon}(x, \alpha)$. By repeating (A1) - (A3) in each domain, we approximate $\bar{c}_i(\alpha)$ for each i. Define the piecewise constant (in x) speed function on Ω by

$$\bar{c}(x, \alpha) = \bar{c}_i(\alpha), \quad x \in \Omega_i.$$

Then proceed as before with the weights assigned as in (B1) using the globally defined speed function $\bar{c}(x, \alpha)$. A numerical example of this kind is considered in §5.2.

Remark. In the periodic medium, the characteristics of the homogenized PDE will be straight lines. In the piecewise-periodic case, the effective Hamiltonian is discontinuous, and the characteristics might change the direction upon crossing the boundary between Ω_i and Ω_j. Nevertheless, for a reasonably small number of subdomains k, the fast sweeping approach will be even more efficient than Dijkstra's method here, since the characteristics rarely switch direction from quadrant to quadrant.

5. Numerical Results

Numerical results and validation are presented in this section. We present homogenization results in several cases where an analytic solution is known. The methods and parameters used in our implementation are described. We numerically validate the first order convergence in ϵ. Finally, we present a result for the three scale problem.

5.1. **Homogenized speed functions.** In this section we compute homogenized speed functions for homogeneous periodic materials, usually piece-wise constant with speeds 1 and 2. Analytical values of $\bar{H}(p)$ given various $c(x)$ can be found in [11] [10] for most examples, and a full description of the checkerboard example can be found in [1].

We compared our numerically computed values $\bar{b}$ with the analytical values of $\bar{H}(p)$ by performing the dual norm calculation numerically using (18)

$$\|q\|_{\bar{b}} = \sup_{|p|=1} \{q \cdot p \mid \bar{H}(p) = 1\},$$

over a discrete set of unit vectors.

All the speed functions are defined on $[-1,1]^2$ and extended periodically.

Example (checkerboard).

$$c^{ch}(x,y) = \begin{cases} c_0 & xy \geq 0, \\ 1 & \text{otherwise.} \end{cases}$$

The exact solution is an octagon for $c_0 \geq c_0^*$,

$$\bar{H}(p_1, p_2) = \frac{c_0}{(\sqrt{2}-1)\min(|p_1|, |p_2|) + \max(|p_1|, |p_2|)}, \quad c_0 \geq c_0^*,$$

and for $c_0 \in [1, c_0^*]$ the solution interpolates between a circle and an octagon, [1]. The plot is for $c_0 = 2$.

Example (Stripes).

$$c^{st}(x) = \begin{cases} 1 & x_2 \in [0,1), \\ 2 & \text{otherwise.} \end{cases}$$

The exact solution for general stripes pattern can be found in [11]. We explain a simple heuristic for computing the cost in this case. The total cost for crossing a large number of stripes is the same even if the pattern is rearranged so that all the slow parts come first and the fast parts second. Then, given a path with slope m, the optimal path will have a corner at the interface and slopes m_1, m_2 in the slow and fast parts, respectively. The optimal path for this configuration can be found by solving for the optimal slopes, which results in Snell's law of refraction.

Example (Squares).

$$c^{sq}(x) = \begin{cases} 1 & x_1 = 0 \text{ or } x_2 = 0, \\ 1/2 & \text{otherwise.} \end{cases}$$

The exact solution is readily seen to be given by a diamond shaped vectogram, since the optimal paths move only in the vertical and horizontal directions.

circle *Example* (Circles).

$$c^{cir}(x) = \begin{cases} 1 & \|x\| \leq 1, \\ 2 & \text{otherwise.} \end{cases}$$

The exact solution is in [10] [11],

$$\bar{H}(p_1, p_2) = \max\left\{|p_1|, |p_2|, \frac{2}{\pi}(|p_1| + |p_2|)\right\}.$$

The optimal paths are made of segments which are either vertical lines, horizontal lines, or quarter circles.

The numerically computed homogenized vectograms are shown in Figure 8, overlaid on the exact result. We also compared the error for a fixed pattern (checkerboard or stripes) but different speed ratios c in the material. The error was computed for a fixed directions as a function of c, and also as a function of the direction for fixed c. See Figures 9 and 10.
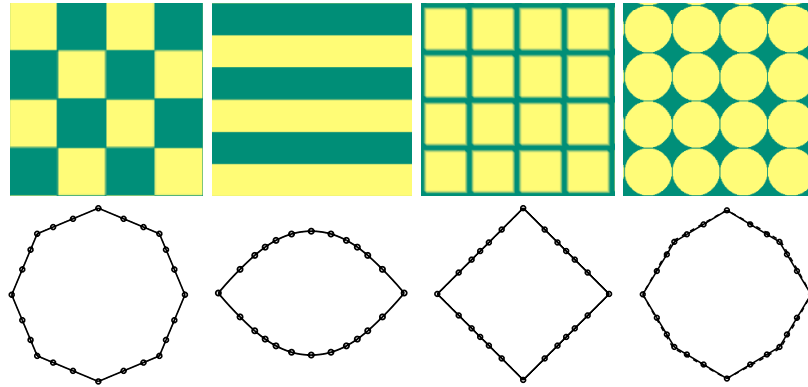

Figure 8: Period domains and computed vectograms: checkerboard, stripes, squares, and circles.   `fig:vectograms`
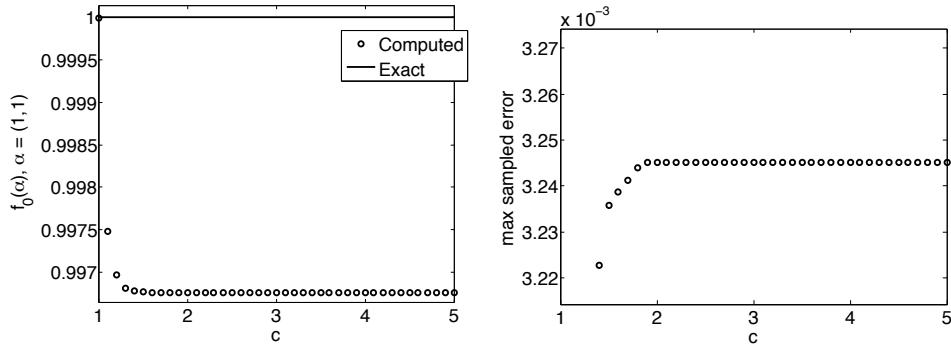

Figure 9: Results using the checkerboard pattern for speeds in $\in [1, 5]$. Left: $\bar{c}(\alpha)$ for $\alpha = (1, 1)$. Right: maximum error over all sampled directions.   `fig:varyChecker`
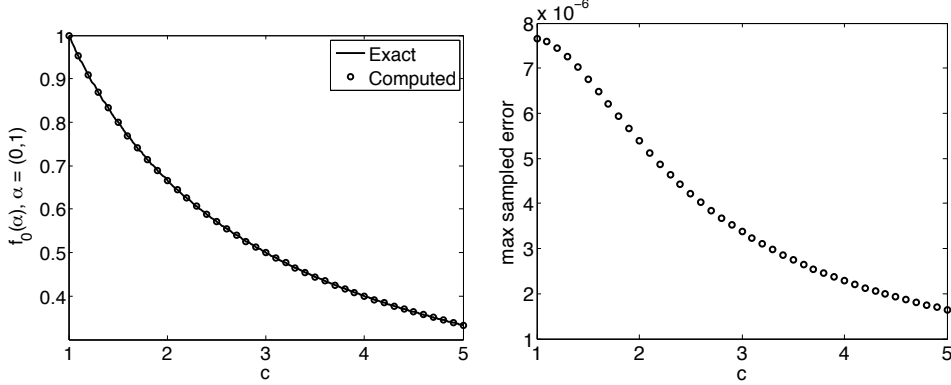
`sec:toy3scale_results`

Figure 10: Results using the horizontal stripes pattern for various speeds in [1, 5]. Left: $\bar{c}(\alpha)$ for the direction $\alpha = (0, 1)$. Right: maximum error over all sampled directions.   `fig:varyHorizontal`

5.2. **The toy three scale problem.** In this section we consider the model problem from §1.4. Consider the following speed function:

$$
c(x) = \begin{cases}
c^{ch}(x) & \text{for } x \in [-1, -\frac{1}{3}]^2 \cup [-\frac{1}{3}, \frac{1}{3}]^2 \cup [\frac{1}{3}, 1]^2, \\
c^{st}(x) & \text{for } x \in [-1, -\frac{1}{3}] \times [-\frac{1}{3}, \frac{1}{3}] \cup [-\frac{1}{3}, \frac{1}{3}] \times [\frac{1}{3}, 1], \\
c^{vert}(x) & \text{for } x \in [-\frac{1}{3}, \frac{1}{3}] \times [-1, -\frac{1}{3}] \cup [\frac{1}{3}, 1] \times [-\frac{1}{3}, \frac{1}{3}], \\
c^{sq}(x) & \text{otherwise.}
\end{cases}
$$

where c^{vert} is the horizontal stripes c^{st} rotated by 90 degrees. We solve for $u^0(x)$ in (HJ^ϵ), in $[-1, 1]^2$ with starting point $(-0.7, -0.7)$. The numerically computed homogenized value function is shown in Figure 11.

5.3. **Methods and parameters used.** We used the first order Fast Marching Method to solve the boundary value problem (HJ^ϵ) for grid size $n = 1200$ and 2400 (so the refinements are h $= 1/600$ and $1/1200$). Then we applied Richardson's extrapolation on h, the spatial resolution, to obtain second order accuracy. The grid directions $\{q_i\}$ were chosen to be the 24 directions on a 7×7 stencil, see Figure 12.

For the connectivity $\mathcal{C}$ of the network, first note that the weights for nodes on the edges of the 7×7 stencil (marked by circles in Figure 12) are known. Then, the weights for all other stencil nodes can be interpolated along the grid direction rays (the weight at the origin is zero), except for nodes not on the grid direction rays. Subsequently, for (B1) - (B3), the local connectivities of the uniformly cartesian network X were chosen to be:

$$\mathcal{C} = \{(ah, bh) : a, b \in \{0, \pm 1, \pm 2, \pm 3\}\} - \{(ah, 2bh), (2ah, bh) : a, b \in \{\pm 1\}\}.$$

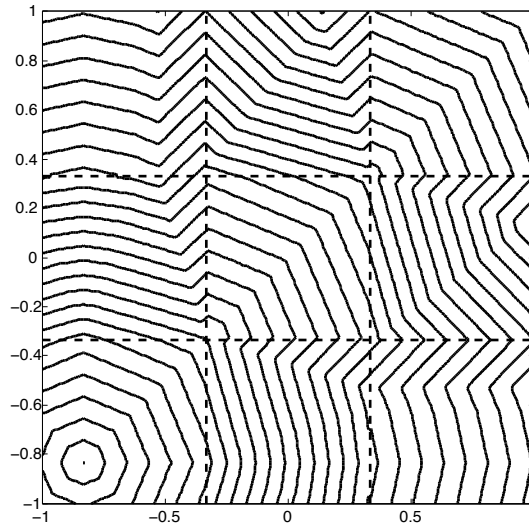The shortest path problem on X was computed using the Fast Sweeping Method.

Figure 11: Level sets of the homogenized solution $T(x)$. The dotted lines $\boxed{\texttt{threeScaleProb}}$ are the interfaces where the periodic pattern changes.
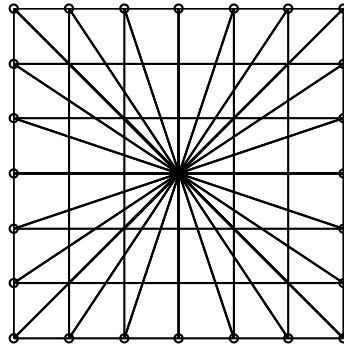

Figure 12: The grid directions $\{q_i\}$. $\boxed{\texttt{fig:24direction}}$

The main script was written in Matlab, and the Fast Marching Method was implemented in C, using code downloaded from [5]. The computations took a few seconds on a desktop computer. The default ratio of fast and slow speed in the cells was 2.

$\boxed{\texttt{justifyextrap}}$

5.4. **Cell and domain resolutions.** In practice, computations were performed for finite values of ϵ. More accurate numerical results were obtained by using Richardson extrapolation for two small values of ϵ. In this situation, there is a trade off between the number of periodic cells on the domain, and the number of grid points in each cell.

We found that accurate results could be obtained by resolving each periodic cell very well, even if a relatively small number of cells were used. Finally, we extrapolated in the spatial resolution h as well. Table 1 compares the errors resulting from different extrapolation choices. Extrapolation in both parameters yields the best accuracy.

Given n (n^2 is the number of grid points used in step (A1).), and ϵ, define the *cell refinement* by

$$n_\epsilon := n\epsilon.$$

The accuracy of our algorithm depends on two parameters: ϵ and n_ϵ. We observed that the convergence rate depends more strongly on n_ϵ, than on ϵ.
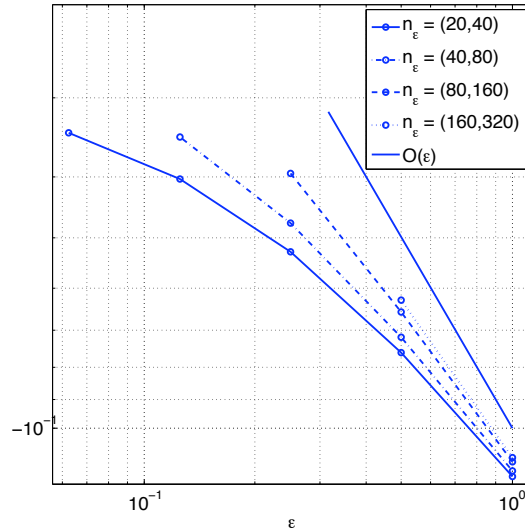

Figure 13: Convergence rate in ϵ for various cell resolutions n_ϵ.

`circleepsiloninterp`

`extrapetable`

pattern	exact $f_0(\alpha)$	error for $h = \epsilon/25, \epsilon/50$ $\epsilon = 1/24$	error for $h = \epsilon/25, \epsilon/50$ $\epsilon = 1/12, 1/24$	error for $h = \epsilon/100, \epsilon/200$ $\epsilon = 1/3, 1/6$
Checkerboard	1	-2.46E-02	-1.64E-02	-3.25E-03
Squares	$1/\sqrt{2}$	9.70E-04	9.65E-04	6.54E-05
Circles	0.90031	-5.10E-02	-4.74E-02	-1.70E-02
Stripes	0.70051	-2.58E-03	-1.53E-02	-1.60E-06

Table 1: Errors in $\bar{c}(\alpha)$ using extrapolation in: h only; h and ϵ (ϵ small); h and ϵ (ϵ large).

Figure 13 shows the convergence rate as a function of ϵ of $\bar{c}(\alpha)$ to the exact $\bar{c}(\alpha)$. We used $\alpha = (\cos(3\pi/4), \sin(3\pi/4))$ for the circle pattern §5.1. Similar results were observed for the other patterns.

In conclusion, the best accuracy is achieved when the two values of ϵ were chosen to be the two largest cell sizes such that the grid directions $\{q_i\}$ all lie on corners of periodic cells, and Richardson's extrapolation is applied. When we used 24 directions, $\{q_i\}$, the best choice was $\epsilon = 1/3$ and $1/6$.

5.5. **Front propagation in random media.** We now consider a random media example. Consider a random checkerboard structure, where in each cell the speed

$$c(x) = \begin{cases} 1 & \text{with probability } 0.5, \\ c_0 > 1 & \text{with probability } 0.5. \end{cases}$$

In this section, computations were performed using higher resolution, but plots use coarser computations for visualization purposes. Sample optimal paths are shown in Figure 4 for two different values of c_0, and with $\epsilon = 1/40$. Experimentally, the homogenized speed $\bar{c}(\alpha)$, averaged over several realizations, is isotropic; the vectogram is a circle. Computations were performed averaging over 20 trials, and sampling 24 sampled directions.

The mean and variance of $\bar{c}$ were computed, as a function of c_0. In each case, the variance was less than 10^{-3}. Figure 14 shows the averaged $\bar{c}(\alpha)$ for $\epsilon = 0.01$ on a 2000^2 grid (but plotted on an 80^2 grid) and the ENO interpolated vectogram with 24 sampled directions, averaged over 20 trials. The dependence of $\bar{c}$ on the value c_0 is also plotted, It was more informative to plot $\bar{b} = 1/\bar{c}$ as a function of $1/c_0$., see Figure 14.

Remark (Average cost in the random case). An upper bound for the homogenized cost is the average of the costs in each cell. This is achieved by paths moving in a straight line in the direction α. But since optimal paths can wander to lower cost cells, the actual computed cost is lower. Better upper bounds can be achieved by estimating the probability that a neighboring cell is low cost. We are not aware of any known formulas for the homogenized speed in this case.

6. CONCLUSIONS

We have introduced a new efficient method for approximating front propagation in periodic multi-scale media. Our approach is based on homogenization of static convex Hamilton-Jacobi equations. We discuss the relationship between several interpretations of such PDEs (from front propagation to time-optimal control to geodesic distance computations). The effective Hamiltonian, resulting from the homogenization, is homogeneous. In more general settings it may vary slowly on the large scale. We include a brief overview of prior methods for homogenization based on solving the cell problem for each direction of front propagation. In contrast, our new
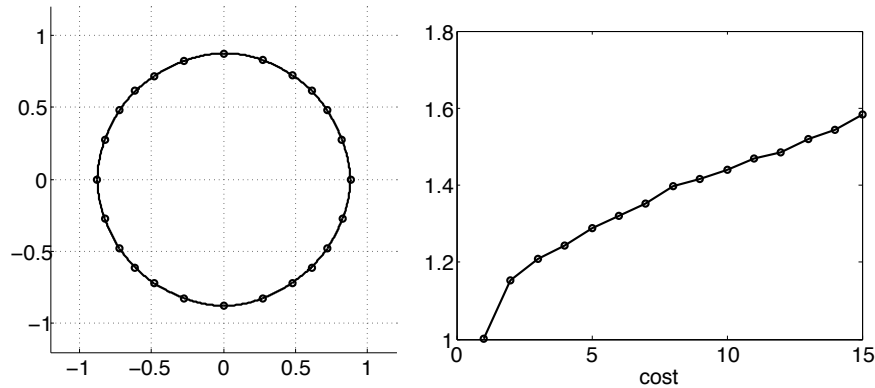
Figure 14: Illustration of the homogenized speed/cost in the random case. `randomMV`
Left: computed vectogram, averaged over several trials, for $c = 1, 1/2$ with
probability $1/2$. Right: computed homogenized cost $\bar{b}$ as a function of the
random cost $b = 1$, or $b = b_0 = 1/c_0$ with probability $1/2$.

`randomConeCircle`

technique uses a single auxiliary boundary value problem to approximate
the homogenized speed of particle motion for all directions. The method
takes advantage of the special structure of the Hamiltonian, and the re-
lationship to the Finsler metric, to compute the homogenized metric, and
then recover the homogenized Hamiltonian. The homogenized metric cost
function and the homogenized particle speed function are related to dual
norms, an equivalent way to relate front speeds and particle speeds is via
the homogeneous Legendre transform. The added advantage of is the ease
of use of semi-Lagrangian numerical schemes on the large scales.

We have illustrated our method with a number of examples of periodic,
piecewise-periodic and random checkerboards. All of these examples start
with an isotropic front propagation on the small scale, but still result in
anisotropic speeds of front propagation after homogenization. Our numerical
algorithm uses a Fast Marching Method [26] to solve an auxiliary (isotropic,
highly-oscillatory) problem to approximate the homogenized particle-speeds
for a finite number of directions, then applies ENO-type interpolation to
complete the speed profile. With the anisotropic particle speed profile in
hand, we then use a variant of Fast Sweeping Method to solve the semi-
Lagrangian discretization of the homogenized Hamilton-Jacobi PDE.

Several extensions of the above approach will be of interest in applica-
tions. First, if the small-scale propagation is anisotropic, we would need to
use Ordered Upwind Methods [28] to approximate the homogenized speed
profiles. Second, if the small-scale behavior is described by a non-convex
Hamiltonian, then our homogenization results do not apply directly, and
new methods are required. Third, if additional length scales are present in

the problem, our methods must be generalized. The toy 3-scale problem considered in this paper is piecewise-periodic, so one homogenized speed profiles was computed for each periodic piece. If instead, the homogenized profile varies continuously on some intermediate scale, any efficient computation on the large scale would require additional interpolation of homogenized speed profiles. Fourth, further exploration of the random case, where we are not aware of analytical solutions. Numerical results suggest the profile is isotropic, and give the homogenized speed as a function of the ratio of the slow and fast speeds for a range of speeds. We intend to address these extensions in the near future.

References

homogChecker

1. M. Amar, G. Crasta, and A. Malusa, *On the finsler metrics obtained as limit of chessboard structures*, available as `http://cvgmt.sns.it/papers/amacramal08/`, 2008.

HomogFinsler

2. M. Amar and E. Vitali, *Homogenization of periodic Finsler metrics*, J. Convex Anal. **5** (1998), no. 1, 171–186. MR MR1649453 (99k:49026)

FinslerBook

3. D. Bao, S.-S. Chern, and Z. Shen, *An introduction to Riemann-Finsler geometry*, Graduate Texts in Mathematics, vol. 200, Springer-Verlag, New York, 2000. MR MR1747675 (2001g:53130)

BardiNotes

4. Martino Bardi, *Some applications of viscosity solutions to optimal control and differential games*, Viscosity solutions and applications (Montecatini Terme, 1995), Lecture Notes in Math., vol. 1660, Springer, Berlin, 1997, pp. 44–97. MR MR1462700 (98f:49029)

bornemann

5. Folkmar Bornemann, *Fast eikonal solver in 2d*, available as `http://www-m3.ma.tum.de/twiki/bin/view/Software/FMWebHome`.

BoydBook

6. Stephen Boyd and Lieven Vandenberghe, *Convex optimization*, Cambridge University Press, Cambridge, 2004. MR MR2061575 (2005d:90002)

BraidesBook

7. Andrea Braides and Anneliese Defranceschi, *Homogenization of multiple integrals*, Oxford Lecture Series in Mathematics and its Applications, vol. 12, The Clarendon Press Oxford University Press, New York, 1998. MR MR1684713 (2000g:49014)

IshiiCD

8. I. Capuzzo-Dolcetta and H. Ishii, *On the rate of convergence in homogenization of Hamilton-Jacobi equations*, Indiana Univ. Math. J. **50** (2001), no. 3, 1113–1129. MR MR1871349 (2002j:35027)

FinslerNotices

9. Shiing-Shen Chern, *Finsler geometry is just Riemannian geometry without the quadratic restriction*, Notices Amer. Math. Soc. **43** (1996), no. 9, 959–963. MR MR1400859 (97e:53129)

concordel

10. Marie C. Concordel, *Periodic homogenisation of Hamilton-Jacobi equations. II. Eikonal equations*, Proc. Roy. Soc. Edinburgh Sect. A **127** (1997), no. 4, 665–689. MR MR1465414 (2000c:35012)

BhattacharyaFronts

11. Bogdan Craciun and Kaushik Bhattacharya, *Homogenization of a Hamilton-Jacobi equation associated with the geometric motion of an interface*, Proc. Roy. Soc. Edinburgh Sect. A **133** (2003), no. 4, 773–805. MR MR2006202 (2004m:35017)

VSCL

12. Michael G. Crandall and Pierre-Louis Lions, *Viscosity solutions of Hamilton-Jacobi equations*, Trans. Amer. Math. Soc. **277** (1983), no. 1, 1–42. MR MR690039 (85g:35029)

Dijkstra

13. E.W. Dijkstra, *A note on two problems in connection with graphs*, Numerische Mathematik **1** (1959), 269–271.

ougandisEngquistReview

14. B. Engquist and P. E. Souganidis, *Asymptotic and numerical homogenization*, Acta Numer. **17** (2008), 147–190. MR MR2436011

`EvansBook`
15. Lawrence C. Evans, *Partial differential equations*, Graduate Studies in Mathematics, vol. 19, American Mathematical Society, Providence, RI, 1998. MR MR1625845 (99e:35001)

`ObermanGomes`
16. Diogo A. Gomes and Adam M. Oberman, *Computing the effective Hamiltonian using a variational approach*, SIAM J. Control Optim. **43** (2004), no. 3, 792–812 (electronic). MR MR2114376 (2006a:49049)

`GremaudKuster`
17. P.A. Gremaud and C.M. Kuster, *Computational study of fast methods for the eikonal equation*, SIAM J. Sc. Comp. **27** (2006), 1803–1816.

`HolmesBook`
18. Mark H. Holmes, *Introduction to perturbation methods*, Texts in Applied Mathematics, vol. 20, Springer-Verlag, New York, 1995. MR MR1351250 (96j:34095)

`HysingTurek`
19. S.-R. Hysing and S. Turek, *The eikonal equation: Numerical efficiency vs. algorithmic complexity on quadrilateral grids*, Proceedings of Algoritmy 2005, 2005, pp. 22–31.

`IsaacsBook`
20. Rufus Isaacs, *Differential games. A mathematical theory with applications to warfare and pursuit, control and optimization*, John Wiley & Sons Inc., New York, 1965. MR MR0210469 (35 #1362)

`BourliouxFronts`
21. Boualem Khouider and Anne Bourlioux, *Computing the effective Hamiltonian in the Majda-Souganidis model of turbulent premixed flames*, SIAM J. Numer. Anal. **40** (2002), no. 4, 1330–1353 (electronic). MR MR1951897 (2003m:76099)

`LionsPapVar`
22. Pierre-Louis Lions, George Papanicolaou, and S.R.S. Varadhan, *Homogenization of Hamilton-Jacobi equations*.

`StuartBook`
23. Grigorios A. Pavliotis and Andrew M. Stuart, *Multiscale methods*, Texts in Applied Mathematics, vol. 53, Springer, New York, 2008, Averaging and homogenization. MR MR2382139

`QianHomog`
24. J Qian, *Two approximations for effective hamiltonians arising from homogenization of Hamilton–Jacobi equations*, http://www.math.ucla.edu/applied/cam/, 2003.

`RorroHomog`
25. M. Rorro, *An approximation scheme for the effective Hamiltonian and applications*, Appl. Numer. Math. **56** (2006), no. 9, 1238–1254. MR MR2244974 (2007e:65093)

`SethianBook`
26. J. A. Sethian, *Level set methods and fast marching methods*, second ed., Cambridge Monographs on Applied and Computational Mathematics, vol. 3, Cambridge University Press, Cambridge, 1999, Evolving interfaces in computational geometry, fluid mechanics, computer vision, and materials science. MR MR1700751 (2000c:65015)

`SethFMM`
27. J.A. Sethian, *A fast marching level set method for monotonically advancing fronts*, Proc. Nat. Acad. Sci. **93** (1996), no. 4, 1591–1595.

`SethianVladOUM`
28. James A. Sethian and Alexander Vladimirsky, *Ordered upwind methods for static Hamilton-Jacobi equations: theory and algorithms*, SIAM J. Numer. Anal. **41** (2003), no. 1, 325–363 (electronic). MR MR1974505 (2004f:65161)

`SoconolfiMetricHJ`
29. Antonio Siconolfi, *Metric character of Hamilton-Jacobi equations*, Trans. Amer. Math. Soc. **355** (2003), no. 5, 1987–2009 (electronic). MR MR1953535 (2005k:35043)

`VladThesis`
30. Alexander Vladimirsky, *Fast methods for static Hamilton-Jacobi Partial Differential Equations*, Ph.D. thesis, University of California, Berkeley, 2001.

`ZhaoFSM`
31. Hongkai Zhao, *A fast sweeping method for eikonal equations*, Math. Comp. **74** (2005), no. 250, 603–627.

DEPARTMENT OF MATHEMATICS, SIMON FRASER UNIVERSITY
E-mail address: aoberman@sfu.ca

DEPARTMENT OF MATHEMATICS, UNIVERSITY OF CALIFORNIA, LOS ANGELES
E-mail address: rrtakei@ucla.edu

DEPARTMENT OF MATHEMATICS, CORNELL UNIVERSITY
E-mail address: vlad@math.cornell.edu